Elafibranor upregulates the EMT-inducer S100A4 via PPARβ/δ

Meijian Zhang, Emma Barroso, Maria Ruart, Lucía Peña, Mona Peyman, David Aguilar-Recarte, Marta Montori-Grau, Patricia Rada, Clara Cugat, Carla Montironi, et al.

Biomedicine & Pharmacotherapy 167 (2023) 115623

Contents lists available at ScienceDirect

Biomedicine & Pharmacotherapy

journal homepage: www.elsevier.com/locate/biopha

Elafibranor upregulates the EMT-inducer S100A4 via PPARβ/δ

Meijian Zhang [a,b,c,1], Emma Barroso [a,b,c,1], Maria Ruart [a,b,c], Lucía Peña [a,b,c], Mona Peyman [a,b,c], David Aguilar-Recarte [a,b,c], Marta Montori-Grau [a,b,c], Patricia Rada [b,d], Clara Cugat [a,b,c], Carla Montironi [e,f], Mohammad Zarei [g,h], Javier Jurado-Aguilar [a,b,c], Antoni Camins [a,i,j], Jesús Balsinde [b,k], Ángela M. Valverde [b,d], Walter Wahli [l,m,n], Xavier Palomer [a,b,c], Manuel Vázquez-Carrera [a,b,c,*]

[a] Department of Pharmacology, Toxicology and Therapeutic Chemistry, Faculty of Pharmacy and Food Sciences and Institute of Biomedicine of the University of Barcelona (IBUB), University of Barcelona, Barcelona, Spain
[b] Spanish Biomedical Research Center in Diabetes and Associated Metabolic Diseases (CIBERDEM)-Instituto de Salud Carlos III, Madrid, Spain
[c] Pediatric Research Institute-Hospital Sant Joan de Déu, Esplugues de Llobregat, Spain
[d] Instituto de Investigaciones Biomédicas Alberto Sols (CSIC/UAM), Madrid, Spain
[e] Pathology Department, Hospital Clínic, Barcelona, Spain
[f] Liver Cancer Translational Research Group, Liver Unit, IDIBAPS-Hospital Clínic, University of Barcelona, Spain
[g] John B. Little Center for Radiation Sciences, Harvard T.H. Chan School of Public Health, Boston, USA
[h] Renal Division, Brigham & Women's Hospital, Harvard Medical School, Boston, USA
[i] Biomedical Research Networking Centre in Neurodegenerative Diseases (CIBERNED), Madrid, Spain
[j] Institute of Neuroscience, University of Barcelona, Barcelona, Spain
[k] Instituto de Biología y Genética Molecular, Consejo Superior de Investigaciones Científicas, Valladolid, Spain
[l] Center for Integrative Genomics, University of Lausanne, CH-1015 Lausanne, Switzerland
[m] Lee Kong Chian School of Medicine, Nanyang Technological University Singapore, 308232, Singapore
[n] INRA ToxAlim, UMR1331, Chemin de Tournefeuille, F-31027 Toulouse Cedex 3, France

ARTICLE INFO

Keywords:
MASLD
Elafibranor
PPARβ/δ
S100A4
ASB2
EMT

ABSTRACT

Elafibranor is a dual peroxisome proliferator-activated receptor (PPAR)α and β/δ agonist that has reached a phase III clinical trial for the treatment of metabolic dysfunction-associated steatotic liver disease (MASLD). Here, we examined the effects of elafibranor in mice fed a choline-deficient high-fat diet (CD-HFD), a model of metabolic dysfunction-associated steatohepatitis (MASH) that presents obesity and insulin resistance. Our findings revealed that elafibranor treatment ameliorated steatosis, inflammation, and fibrogenesis in the livers of CD-HFD-fed mice. Unexpectedly, elafibranor also increased the levels of the epithelial-mesenchymal transition (EMT)-promoting protein S100A4 via PPARβ/δ activation. The increase in S100A4 protein levels caused by elafibranor was accompanied by changes in the levels of markers associated with the EMT program. The S100A4 induction caused by elafibranor was confirmed in the BRL-3A rat liver cells and a mouse primary hepatocyte culture. Furthermore, elafibranor reduced the levels of ASB2, a protein that promotes S100A4 degradation, while ASB2 overexpression prevented the stimulating effect of elafibranor on S100A4. Collectively, these findings reveal an unexpected hepatic effect of elafibranor on increasing S100A4 and promoting the EMT program.

Abbreviations: ASB2, ankyrin repeat and suppressor of cytokine signaling box containing 2 protein; CD-HFD, choline-deficient high-fat diet; COL1A1, collagen type I α1; CRISPR/dCas9, clustered regularly interspaced short palindromic repeats/deactivated CRISPR-associated protein 9; EMT, epithelial-mesenchymal transition; ERK, extracellular signal-regulated kinases; FSP1, fibroblast-specific protein 1; GTT, glucose tolerance test; ITT, insulin tolerance test; MASLD, metabolic dysfunction-associated steatotic liver disease; MASH, metabolic dysfunction-associated steatohepatitis; PPAR, peroxisome proliferator-activated receptor; siRNA, small interfering RNA; α-SMA, α-smooth muscle actin; S100A4, S100 calcium binding protein A4; 16:0/18:1-PC, 1-palmitoyl-2-oleoyl-sn-glycero-3-phosphocholine.

* Correspondence to: Unitat de Farmacologia, Facultat de Farmàcia i Ciències de l'Alimentació, Av. Joan XXIII 27-31, E-08028 Barcelona, Spain.
E-mail address: mvazquezcarrera@ub.edu (M. Vázquez-Carrera).

[1] Both authors contributed equally

https://doi.org/10.1016/j.biopha.2023.115623
Received 20 June 2023; Received in revised form 27 September 2023; Accepted 28 September 2023
Available online 30 September 2023

1. Introduction

Metabolic dysfunction-associated steatotic liver disease (MASLD) is the most common cause of chronic liver disease in individuals without significant alcohol consumption. Its major drivers are obesity and insulin resistance. The global prevalence of MASLD in the general population is 25% [1], with this percentage increasing to 90% in subjects with morbid obesity [2]. MASLD ranges from hepatic steatosis (without hepatocyte injury in the form of hepatocyte ballooning) to a more severe condition known as metabolic dysfunction-associated steatohepatitis (MASH, steatosis with ballooning, inflammation, with or without fibrosis). MASH increases the risk of developing more serious diseases such as cirrhosis, hepatocellular carcinoma (HCC), and cardiovascular disease [3–5].

Although many pharmacotherapies are being evaluated for the treatment of MASH, there are currently no US Food and Drug Administration (FDA) approved specific pharmacological drugs for the treatment of this condition. As a result, given the complexity of its pathophysiology, the best treatment for this disease might be the use of compounds activating several targets or a combination of drugs targeting different mechanistic pathways [6]. Following this rationale, elafibranor (also known as GFT505), a dual peroxisome proliferator-activated receptor α (PPARα) and β/δ agonist was developed, and has reached a phase III clinical trial. In humans, elafibranor was observed to show a modest effect on the histological resolution of MASH, but did not demonstrate any significant effect on fibrosis [7], the main driver of all-cause and liver-related mortality in MASH patients [8]. As a result, elafibranor was discontinued in 2020 because it did not meet the predefined primary surrogate endpoint of MASH resolution without the worsening of fibrosis [9]. Despite this negative outcome, the efficacy of elafibranor will be evaluated in combination with other drugs for the treatment of MASH [10]. In PPARα knockout mice, elafibranor prevents liver steatosis and inflammation, suggesting that these actions are mediated by PPARβ/δ activation [11]. PPARβ/δ is expressed in the main liver cell types (hepatocytes, Kupffer cells, cholangiocytes and hepatic stellate cells) [12] and its activation hinders the progression of MASLD by ameliorating insulin resistance, reducing lipogenesis, and alleviating inflammation and endoplasmic reticulum stress [13]. However, the use of PPARβ/δ agonists as therapeutic agents needs to be performed with caution as the activation of this nuclear receptor may have tumorigenic effects, although the role of PPARβ/δ in cancer is controversial [14].

An important process propagating the progression of liver fibrosis is the epithelial-mesenchymal transition (EMT). This is a program by which epithelial cells, such as hepatocytes and cholangiocytes, lose their epithelial phenotype (polarity and adherence) and acquire mesenchymal characteristics (motility and invasiveness) [15]. Hepatocyte EMT is induced by transforming growth factor β (TGF-β) and carbon tetrachloride (CCl_4), and is characterized by the downregulation of epithelial markers (e.g. E-cadherin) and the upregulation of mesenchymal markers such as vimentin and S100 calcium binding protein A4 (S100A4, also known as fibroblast-specific protein 1, FSP1). Indeed, S100A4 is considered an inducer of the EMT program [16]. Interestingly, S100A4-knockout mice fed a methionine-choline-deficient (MCD) diet show attenuated liver fibrosis and inflammation, as well as an inhibition of hepatocyte apoptosis [17]. S100A4 also seems to play a role in liver tumorigeneses, since S100A4-deficient mice develop significantly fewer and smaller liver tumor nodules, while showing decreases in liver fibrosis and the expression of stem cell markers in the HCC tissues [15]. In fact, increased S100A4 protein levels correlate with poor prognosis in several cancers, with S100A4 promoting the development of metastasis in mouse models of cancer [17]. The effects of S100A4 have been associated with the formation of oligomers of this protein, which is stimulated by oxidation [18]. Moreover, S100A4 does not possess enzymatic activity, but rather interacts with target proteins and regulates their activity. Intracellular targets of S100A4 include p53 and non-muscle myosin IIA (NMIIA) [19]. Overall, these findings suggest that S100A4 is a regulator of both fibrogenesis and tumorigenesis in the liver.

In the present study, we examined the effects of elafibranor in mice fed a choline-deficient high-fat diet (CD-HFD), a model of MASH that presents obesity and insulin resistance and thus closely resembles human MASH [20,21]. Elafibranor treatment improved steatosis, inflammation, and fibrogenesis in these mice, but, surprisingly, it increased protein level of the EMT-inducer S100A4 through PPARβ/δ activation and this increase was accompanied by changes in the levels of the markers associated with the EMT program. Our findings also revealed that elafibranor reduced levels of the S100A4-degrading E3 ubiquitin ligase, ankyrin repeat and suppressor of cytokine signaling box containing protein 2 (ASB2). Likewise, the increased S100A4 levels caused by elafibranor was prevented by the overexpression of ASB2, indicating that the reduction of this E3 ubiquitin ligase is the underlying mechanism involved in S100A4 upregulation. Overall, these findings indicate that PPARβ/δ is a new player in the control of hepatic EMT in mice, with potential implications in the regulation of MASH development and the promotion of liver tumors.

2. Materials and methods

2.1. Reagents

Control siRNA and S100A4 siRNA were purchased from Santa Cruz (Dallas, TX, USA). GW501516, GSK0660 and U0126 were purchased from Sigma-Aldrich (Madrid, Spain) and elafibranor from AXON Medchem (Groningen, the Netherlands).

2.2. Mice

Male C57BL/6 mice (10–12 weeks old) (Envigo, Barcelona, Spain) were housed and maintained under a constant temperature (22 ± 2 °C) and humidity (55%). The mice had free access to water and food and were subjected to 12-h light-dark cycles. After 1 week of acclimatization, the mice were randomly distributed into three experimental groups (n = 6 each) and fed either standard chow (one group) or a choline-deficient high-fat diet (CD-HFD; 44.9 kcal% fat, 35.1 kcal% carbohydrates, and 20.0 kcal% protein, without added choline; D05010402, Research diets, New Brunswick, NJ, USA) (two groups) for 12 weeks. Mice fed standard chow and one of the groups of mice fed the CD-HFD received one daily p.o. gavage of vehicle (0.5% w/v carboxymethylcellulose), while the remaining group fed the CD-HFD received one daily p.o. dose of 10 mg/kg/day of elafibranor dissolved in the vehicle (volume administered, 1 ml/kg) during the last 4 weeks. In a second study, the mice were randomly distributed in three experimental groups (n = 6 each) and fed either standard chow (one group) or the CD-HFD (D05010402, Research Diets) for 12 weeks. Mice fed standard chow and one of the groups fed the CD-HFD received one daily p.o. gavage of vehicle (0.5% w/v carboxymethylcellulose), while the remaining group fed the CD-HFD received one daily p.o. dose of 5 mg/kg/day of the PPARβ/δ agonist GW501516 dissolved in the vehicle (volume administered, 1 ml/kg) during the last 4 weeks. At the end of the treatment, the mice were sacrificed, and liver samples were frozen in liquid nitrogen and then stored at − 80ºC. In a third study, male (8–9 weeks old) *Ppard*-knockout (*Ppard*$^{-/-}$) mice (n = 6) and their wild-type littermates (*Ppard*$^{+/+}$) (n = 6) with the same genetic background (C57BL/6 ×129/SV) [50], all fed a control diet, were used. The mice were sacrificed, and liver samples were frozen in liquid nitrogen and then stored at − 80ºC.

For the glucose tolerance test (GTT) and insulin tolerance test (ITT), the animals received 2 g/kg body weight of glucose and 0.75 IU/kg body weight of insulin respectively through an intraperitoneal injection. Blood was collected from the tail at 0, 15, 30, 60, and 120 min

All experiments were performed in accordance with European Community Council directive 86/609/EEC. The experimental protocols

as well as the number of animals, determined based on the expected effect size, were approved by the Institutional Animal Care and Use Committee of the University of Barcelona. The reporting of the animal studies complied with the ARRIVE guidelines [51].

2.3. Liver histology

For histological staining studies, 4-μm sections obtained from formalin-fixed paraffin-embedded samples were stained with hematoxylin and eosin (H&E) to assess liver histology, as well as Sirius Red to assess fibrosis. Oil Red O staining (Sigma-Aldrich) to assess lipid content was performed in frozen 10-μm liver sections. Fifteen images at a magnification of 20x were captured to quantify the red-stained collagen or lipid droplets, with the red-stained area evaluated per total area using Image J.

2.4. Analysis of 1-palmitoyl-2-oleoyl-sn-glycero-3-phosphocholine (16:0/18:1-PC)

Total lipids from liver homogenates were extracted according to Bligh and Dyer [52], evaporated, and redissolved in methanol-water (9:1). Total lipid separation, identification, and quantification were carried out by liquid chromatography/mass spectrometry using a Hitachi LaChrom Elite L-2130 binary pump and a Hitachi autosampler L-2200 (Merck, Darmstadt, Germany) coupled to a Bruker esquire6000 ion-trap mass spectrometer [53]. The effluent was split, entering at 0.2 ml/min into the electrospray interface of the mass spectrometer. The nebulizer was set to 30 ψ, the dry gas to 8 l/min, and the dry temperature to 350ºC. A Supelcosil LC-18 column of 5 μm particle size, measuring 250 × 2.1 mm and with a particle size of 5 μm (Sigma-Aldrich) was used, protected with by a Supelguard LC-18 guard cartridge column measuring 20- × 2.1 -mm guard cartridge column (Sigma-Aldrich). The mobile phase used was a gradient of solvent A [methanol/water/hexane/ammonium hydroxide, 87.5:10.5:1.5:0.5 (vol/vol/vol/vol)], solvent B [methanol/hexane/ammonium hydroxide, 87.5:12:0.5 (vol/vol/vol)], and solvent C [methanol/water, 9:1 (vol/-vol)]. The gradient started at 100% A, decreased linearly to 50% A (50% B) in 17.5 min and to 0% A (100% B) in 12.5 min, before being maintained at 100% B for 5 min, changed to 100% C in 3 min, maintained at 100% C for 9 min, and then changed to 100% B in 3 min. The flow rate was 0.5 ml/min and the injection volume was 80 μl. Data acquisition was carried out in the full scan and positive mode, detecting PC species as $[M^{+}H]^{+}$ ions with the capillary current set at − 4000 V. The PC (16:0/18:1) species were characterized by tandem mass spectrometry in the multiple reaction monitoring and negative mode, with a postcolumn addition of acetic acid for [M + CH3CO2]-adduct formation (100 μl/h). 1,2-Dinonadecanoyl-sn-glycero-3-phosphocoline (m/z = 818.6) was used as the internal standard and in a calibration curve for quantification.

2.5. Cell culture

The rat hepatocyte cell line BRL-3 A (P9–13, RRID:CVCL_0606) was purchased from the European Collection of Authenticated Cell Cultures (ECACC, Salisbury, United Kingdom). Cells were cultured under standard culture conditions (37 °C, 5% CO_2) in Dulbecco's Modified Eagle Medium (DMEM) supplemented with 10% fetal bovine serum (FBS) and 1% penicillin/streptomycin. BRL-3 A cells were incubated in serum-free DMEM in the absence (control cells) or presence of elafibranor (different concentrations), U0126 (different concentrations), GW501516 (10 μM), or GSK0660 (60 μM).

BRL-3A cells were transiently transfected with 100 nM siRNA against S100A4 or the control siRNA in Opti-MEM medium (Thermo Fisher, MA, USA) using Lipofectamine 2000 (Invitrogen, Carlsbad, CA, USA) (13.2 μl per 2.2-ml well) according to the manufacturer's instructions.

Mouse primary hepatocytes were isolated from non-fasting male C57BL/6 mice (10–12 weeks old) by perfusion with collagenase, as described elsewhere [54], and incubated in either the absence (control cells) or presence of drugs (elafibranor or GW501516).

All the cell experiments were repeated at least 4 times and there were 2 replicates in each experiment.

2.6. Transfection of the Asb2 CRISPR/dCas9 activation plasmids in BRL-3A cells

To overexpress *Asb2* in the BRL-3A cells, the CRISPR/dCas9 activation system was used. The *Asb2* CRISPR/dCas9 activation plasmid (sc-425766-ACT; Santa Cruz Biotechnology) consisted of a pool of three plasmids designed to overexpress the *Asb2* gene. The control CRISPR/dCas9 activation plasmid (sc-437275; Santa Cruz Biotechnology) was used as a negative control. Plasmid transfection medium and Lipofectamine 2000 were used according to the manufacturer's protocol. Briefly, cells (1×10^5 cells per well) were seeded in 6-well culture plates of 1.5 ml antibiotic-free DMEM 24 h before transfection and grown to 50–60% confluence. Cells were transfected with 1.5 μg of the *Asb2* CRISPR/dCas9 activation system (Santa Cruz Biotechnology), using Lipofectamine 2000 in Opti-MEM medium (Santa Cruz Biotechnology) and incubated at 37ºC with 5% CO_2. Three days after transfection, the cells were used for evaluation.

2.7. Reverse transcription-polymerase chain reaction and quantitative polymerase chain reaction

Isolated RNA was reverse transcribed to obtain 1 μg of complementary DNA (cDNA) using Random Hexamers (Thermo Scientific), 10 mM deoxynucleotide (dNTP) mix and the reverse transcriptase enzyme derived from the Moloney murine leukemia virus (MMLV, Thermo Fisher). The experiment was run in a thermocycler (BioRad) and consisted of a program with different steps and temperatures: 65 °C for 5 min, 4 °C for 5 min, 37 °C for 2 min, 25 °C for 10 min, 37 °C for 50 min, and 70 °C for 15 min. The relative levels of specific mRNAs were assessed by real-time RT-PCR in a Mini 48-Well T100™ thermal cycler (Bio-Rad), using the SYBR Green Master Mix (Applied Biosystems), as previously described [55]. Briefly, samples had a final volume of 20 μl, with 20 ng of total cDNA, 0.9 μM of the primer mix, and 10 μl of 2x SYBR Green Master Mix. The thermal cycler protocol for real-time PCR included a first step of denaturation at 95 °C for 10 min followed by 40 repeated cycles of 95 °C for 15 s, 60 °C for 30 s, and 72 °C for 30 s for denaturation, primer annealing, and amplification respectively. Primer sequences were designed using the Primer-BLAST tool (NCBI), based on the full mRNA sequences to find the optimal primers for amplification, and evaluated with the Oligo-Analyzer Tool (Integrated DNA Technologies) to ensure an optimal melting temperature (Tm) and avoid the formation of homo/heterodimers or non-specific structures that can interfere with the interpretation of the results. The primer sequences were designed specifically to span the junction between the exons. The primer sequences used are provided in Supplementary Table 1. Values were normalized to the glyceraldehyde 3-phosphate dehydrogenase (*Gapdh*) or adenine phosphoribosyltransferase (*Aprt*) expression levels, and measurements were performed in triplicate. All changes in expression were normalized to the untreated control.

2.8. Immunoblotting

The isolation of total protein extracts was performed as described elsewhere [25]. Immunoblotting was performed with antibodies against β-actin (Sigma, A5441), E-cadherin (Santa Cruz, sc-8426), COL1A1 (Cell Signaling, 91144 S), phosphorylated (p)44/42 MAPK (Erk1/2) (Cell Signaling, 9194 s), phosphorylated (p) p44/42 MAPK (Erk1/2) Thr202/Tyr204 (Cell Signaling, 9101 s), filamin A (Santa Cruz, sc-376241), GAPDH (G-9) (Santa Cruz, sc-365062), α-SMA (Invitrogen, 14–9760–82), S100A4/FSP1 (EMD Millipore, o7–2274), α-tubulin

(Sigma, T6074), and vimentin (Santa Cruz, sc-6260). The serum raised against a peptide common to the ASB2α and ASB2β isoforms was provided by C. Moog-Lutz (IPBS, Toulouse, France) [32]. Signal acquisition was conducted using the Bio-Rad ChemiDoc apparatus and quantification of the immunoblot signal was performed with the Bio-Rad Image Lab software. The results for protein quantification were normalized to the levels of a control protein (GAPDH, α-tubulin or β-actin) to avoid unwanted sources of variation.

2.9. Statistical analysis

Results are expressed as the mean ± SEM. Significant differences were assessed by either Student's t-test or one-way and two-way ANOVA, according to the number of groups compared, using the GraphPad Prism program (version 9.0.2) (GraphPad Software Inc., San Diego, CA, USA). When significant variations were found by ANOVA, Tukey's post-hoc test for multiple comparisons was performed only if F achieved a p value < 0.05. Differences were considered significant at $p < 0.05$.

3. Results

3.1. The dual PPARα and β/δ agonist elafibranor improves MASLD, but upregulates hepatic S100A4 levels in mice fed a CD-HFD

First, we evaluated the effects of elafibranor on body weight and glucose metabolism. Elafibranor treatment did not reduce the body weight gain caused by the CD-HFD, but it did improve the glucose intolerance and peripheral insulin resistance caused by the CD-HFD (Fig. 1A-C). Although PPARβ/δ activation has been reported to increase hepatic levels of the PPARα endogenous ligand 1-palmitoyl-2-oleoyl-sn-glycero-3-phosphocholine (16:0/18:1-PC) [22], it is unknown whether elafibranor affects the amount of this ligand that may potentiate the beneficial actions of the drug via PPARα. We found that the CD-HFD did not affect hepatic levels of 16:0/18:1-PC (Fig. 1D). However, elafibranor markedly increased the levels of this PPARα ligand in the liver. This effect of elafibranor has been reported previously for the PPARβ/δ activator GW501516 [23]. Therefore, the fact that 16:0/18:1-PC levels were reduced in the livers of *Ppard*$^{-/-}$ mice compared with wild-type (WT) mice (Fig. 1E) suggests that the effect of elafibranor on 16:0/18:1-PC levels is mediated by PPARβ/δ. These findings indicate that elafibranor, besides its direct effect on PPARα, may also indirectly activate this nuclear receptor by increasing the amount of 16:0/18:1-PC. Since fibroblast growth factor 21 (FGF21) is a target in the treatment of MASH and given that PPARα activation increases its levels [24], we determined the hepatic mRNA levels of FGF21. The CD-HFD did no present a significant increase in *Fgf21* mRNA levels, whereas treatment with elafibranor significantly raised *Fgf21* expression (Fig. 1F).

Hematoxylin-eosin and Oil Red O (ORO) staining showed that the CD-HFD caused significant hepatic lipid accumulation, which was reduced by elafibranor (Fig. 2A-B). The CD-HFD led to a non-significant increase in the accumulation of collagen in the liver, as demonstrated by the Sirius Red staining, suggesting that a longer exposure to the CD-HFD is required to induce clear fibrosis. Notably, elafibranor decreased collagen accumulation (Fig. 2C). Consistent with findings of the Sirius Red staining, the CD-HFD did not significantly increase the protein levels of the fibrosis markers α-smooth muscle actin (α-SMA) and collagen type I α1 (COL1A1), but treatment with elafibranor caused a significant reduction of their levels (Fig. 2D-E).

When we examined the effects of elafibranor on *S100A4* expression, we observed that the CD-HFD in mice treated with vehicle and in those administered elafibranor did not significantly affect the mRNA levels of this gene (Fig. 3A). The S100A4 protein can be detected either as a monomer or a dimer, the latter being S-glutathionylated, with apparent molecular weights of 11.5 kDa and approximately 21–29 kDa respectively [25,26]. No changes were observed in the hepatic protein levels of S100A4 in mice fed the CD-HFD. By contrast, mice fed the CD-HFD and treated with elafibranor displayed a robust increase in the protein with a molecular weight of ~ 23 kDa (Fig. 3B). The effect of elafibranor on S100A4 was probably the result of PPARβ/δ activation, since the mice treated with the selective agonist for this receptor, GW501516, also showed increased hepatic protein levels of S100A4 (Fig. 3C). Moreover, the band corresponding to S100A4 was reduced in the livers of *Ppard*$^{-/-}$ mice compared to their wild-type littermates, indicating that S100A4 is regulated by PPARβ/δ (Fig. 3D). Since an increase in the mesenchymal marker S100A4 might indicate that elafibranor activates the EMT program, we analyzed other markers of this program such as the epithelial marker E-cadherin and the mesenchymal marker vimentin. In agreement with the increase in S100A4 levels and the subsequent induction of the EMT program, elafibranor reduced the protein levels of E-cadherin and increased those of vimentin (Fig. 3E, F). These findings suggest that PPARβ/δ activation by elafibranor increases the hepatic protein levels of S100A4 and activates the EMT program in the liver.

3.2. Elafibranor increases S100A4 protein levels in BRL-3A rat liver cells and in a mouse primary hepatocyte culture

Treatment of the rat liver cell line BRL-3A with either GW501516 (a selective agonist of PPARβ/δ at concentrations of up to 10 μM [27]), or elafibranor (at a concentration of 30 or 60 μM) did not increase S100A4 mRNA levels compared to control cells (Fig. 4A). By contrast, elafibranor at both concentrations increased S100A4 protein levels, whereas GW501516 had no effect (Fig. 4B). The S100A4 protein upregulated by elafibranor in the rat BRL-3A cells showed a higher molecular weight than that detected in mice, suggesting interspecies differences in the S-glutathionylation of this protein [28]. S100A4 knockdown by siRNA transfection in the BRL-3A cells caused a reduction in the protein levels of S100A4, confirming that the protein band detected was S100A4 (Supplementary Figure 1 A). Elafibranor at 60 μM reduced E-cadherin protein levels (Fig. 4C) and increased vimentin protein levels (Fig. 4D), while GW501516 only increased vimentin levels without affecting E-cadherin levels (Fig. 4C, D). The increase in S100A4 protein levels caused by elafibranor was prevented by the PPARβ/δ antagonist GSK0660 (Fig. 4E), confirming the involvement of PPARβ/δ in the changes caused by its activation. The effects of elafibranor were confirmed in a mouse primary culture of hepatocytes, where elafibranor increased S100A4 protein levels (Fig. 4F). In these primary hepatocytes, GW501516 increased S100A4 protein levels, in contrast to the observations in the BRL-3A cells, suggesting that the primary hepatocytes respond better than the rat BRL-3A cells (Fig. 4G). Overall, these findings indicate that elafibranor increases the protein levels of S100A4 in hepatocytes via PPARβ/δ.

3.3. Elafibranor increases S100A4 by reducing the protein levels of the E3 ubiquitin ligase ASB2

Next, we examined whether, as suggested by the results above, there was a potential post-transcriptional mechanism by which elafibranor increased S100A4 protein levels. Since reactive oxygen species (ROS) modify S100A4 activity and dimerization [20], we explored the involvement of ROS in the effects of elafibranor. Under our conditions, the incubation of BRL-3A cells with H_2O_2 or the co-incubation of elafibranor-exposed cells with the antioxidant N-acetylcysteine did not affect S100A4 protein levels, indicating that ROS were not involved (Supplementary Figure 1B).

Interestingly, it has been reported that the inhibition of the activities of extracellular signal- regulated kinases 1 and 2 (ERK1/2) reduces the activity of several E3 ubiquitin ligases [29]. Since we have previously reported that PPARβ/δ activation inhibits ERK1/2 activity [30], we evaluated whether the inhibition of this kinase mediated the effects of

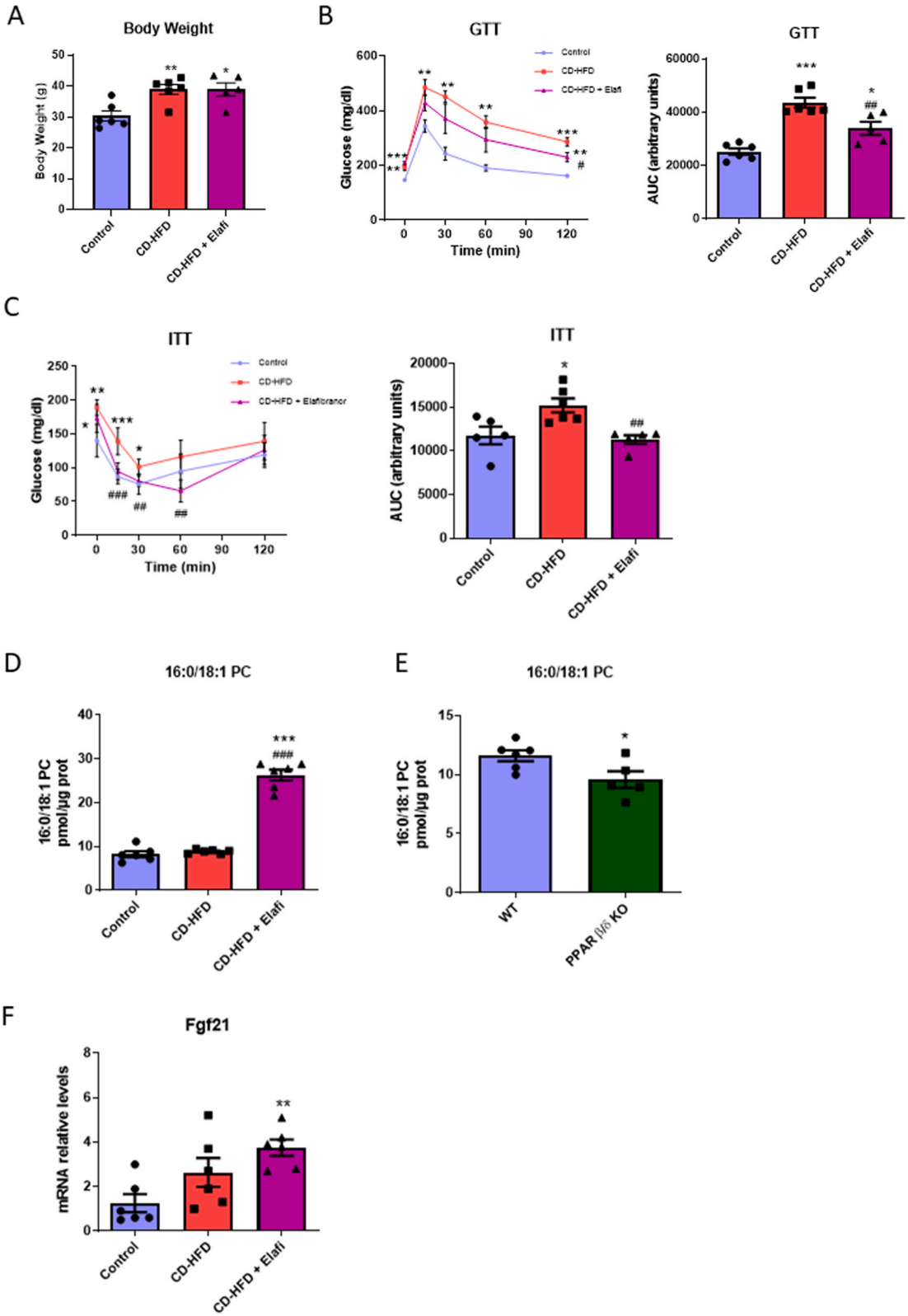

Fig. 1. Elafibranor improves insulin sensitivity in mice fed a CD-HFD. (**A**) Final body weight in mice (n = 6 animals) fed a standard diet (control) or a choline-deficient high-fat diet (CD-HFD) for 12 weeks and treated with vehicle or 10 mg/kg/day of elafibranor during the last 4 weeks. (**B**) Glucose tolerance test (GTT) and area under the curve (AUC) (n = 6 animals). (**C**) Insulin tolerance test (ITT) and AUC (n = 6 animals). (**D**) Hepatic levels of the PPARα endogenous ligand 1-palmitoyl-2-oleoyl-sn-glycero-3-phosphocholine (16:0/18:1-PC). (**E**) 16:0/18:1-PC hepatic levels in wild-type (WT) and *Ppard*$^{-/-}$ mice (n = 5 animals). (**F**) *Fgf21* mRNA levels in mice (n = 6 animals) fed a standard diet (control) or a CD-HFD and treated with vehicle or 10 mg/kg/day of elafibranor during the last 4 weeks. Data are presented as the mean ± SEM. *$p < 0.05$, * *$p < 0.01$, and * **$p < 0.001$ versus control or WT. $^{\#\#}p < 0.01$ and $^{\#\#\#}p < 0.001$ versus CD-HFD-fed mice. p-values determined by one-way ANOVA with Tukey's post hoc test (A, B, C, D, and F) or two-tailed unpaired Student's t-test (E).

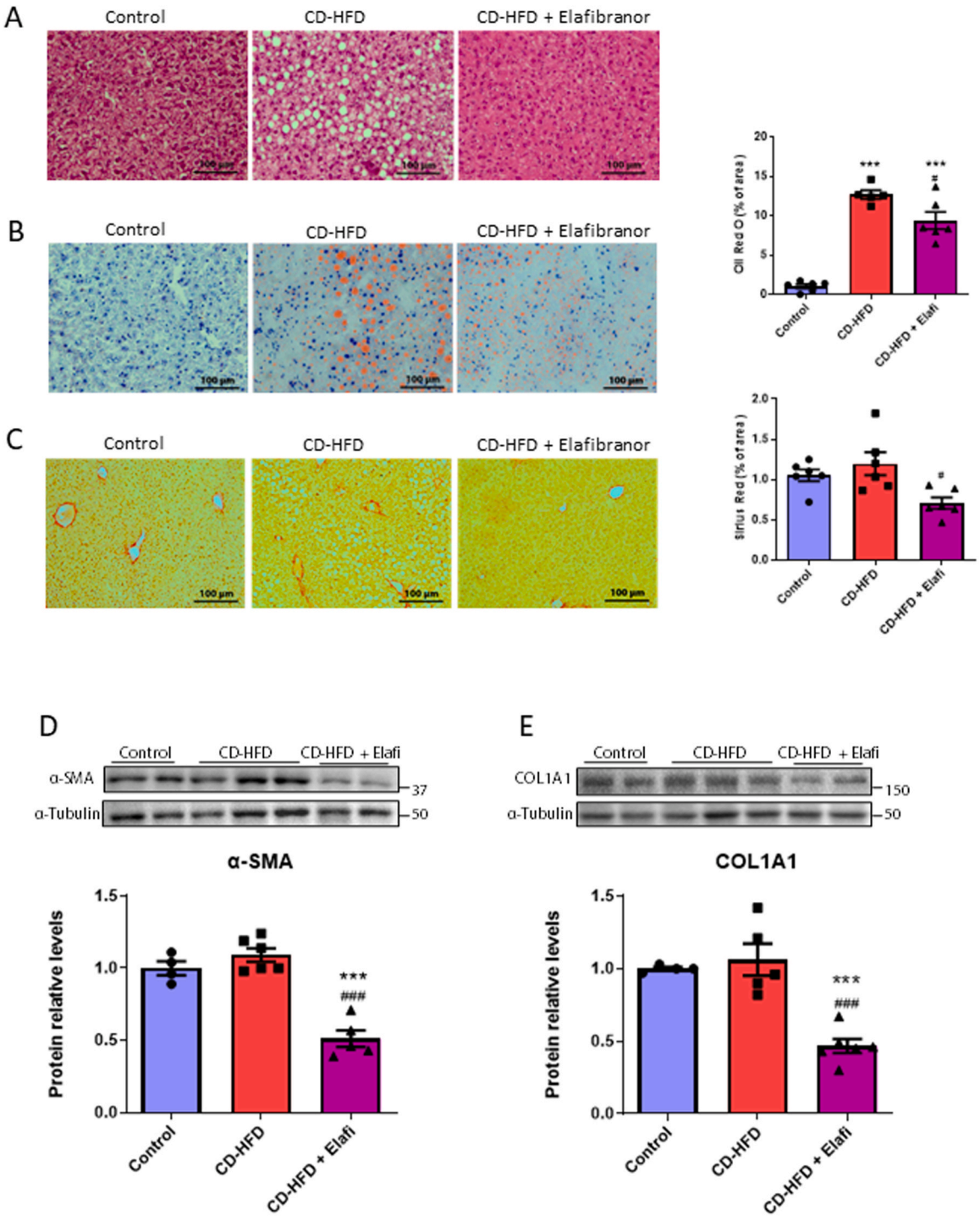

Fig. 2. Elafibranor decreases markers of fibrosis in mice fed a CD-HFD. (**A**) Hematoxylin–eosin (H&E), (**B**) Oil Red O (ORO) and (**C**) Sirius Red staining of liver sections and quantification of ORO and Sirius Red staining of samples from mice (n = 6 animals) fed a standard diet (control) or a choline-deficient high-fat diet (CD-HFD) for 12 weeks and treated with vehicle or 10 mg/kg/day of elafibranor during the last 4 weeks. Scale bar: 100 μm. Liver cell lysate extracts were assayed via western blot analysis with antibodies against α-SMA (**D**) and COL1A1 (**E**) (n = 6 animals). Data are presented as the mean ± SEM. *$p < 0.05$ versus control. $^{\#}p < 0.05$, $^{\#\#}p < 0.01$, and $^{\#\#\#}p < 0.001$ versus CD-HFD-fed mice. p-values determined by one-way ANOVA with Tukey's post hoc test.

elafibranor on S100A4. Consistent with the previous findings reported for PPARβ/δ activation [30,31], elafibranor reduced phosphorylated ERK1/2 levels in the livers of mice fed the CD-HFD (Fig. 5A). However, the ERK1/2 inhibitor U0126, which reduced phosphorylated ERK1/2 levels even more than elafibranor (Fig. 5B), did not increase the protein levels of S100A4 in the BRL-3A cells (Fig. 5C), thereby indicating that ERK1/2 inhibition was not the mechanism responsible for the elafibranor-induced increase in S100A4 levels.

ASB2β is the specificity subunit of a multimeric E3 ubiquitin ligase [32] that has been reported to induce the degradation of S100A4 [31]. We therefore speculated that the increased S100A4 protein levels induced by elafibranor were due to a reduced expression of ASB2β. In the protein lysates of both mouse livers and BRL-3A cells, a 70-kDa band corresponding to ASB2β was detected with an antibody raised against a peptide common to both the ASB2α and ASB2β isoforms (Fig. 6A, B). The amount of this protein was reduced in the livers of the CD-HFD-fed mice

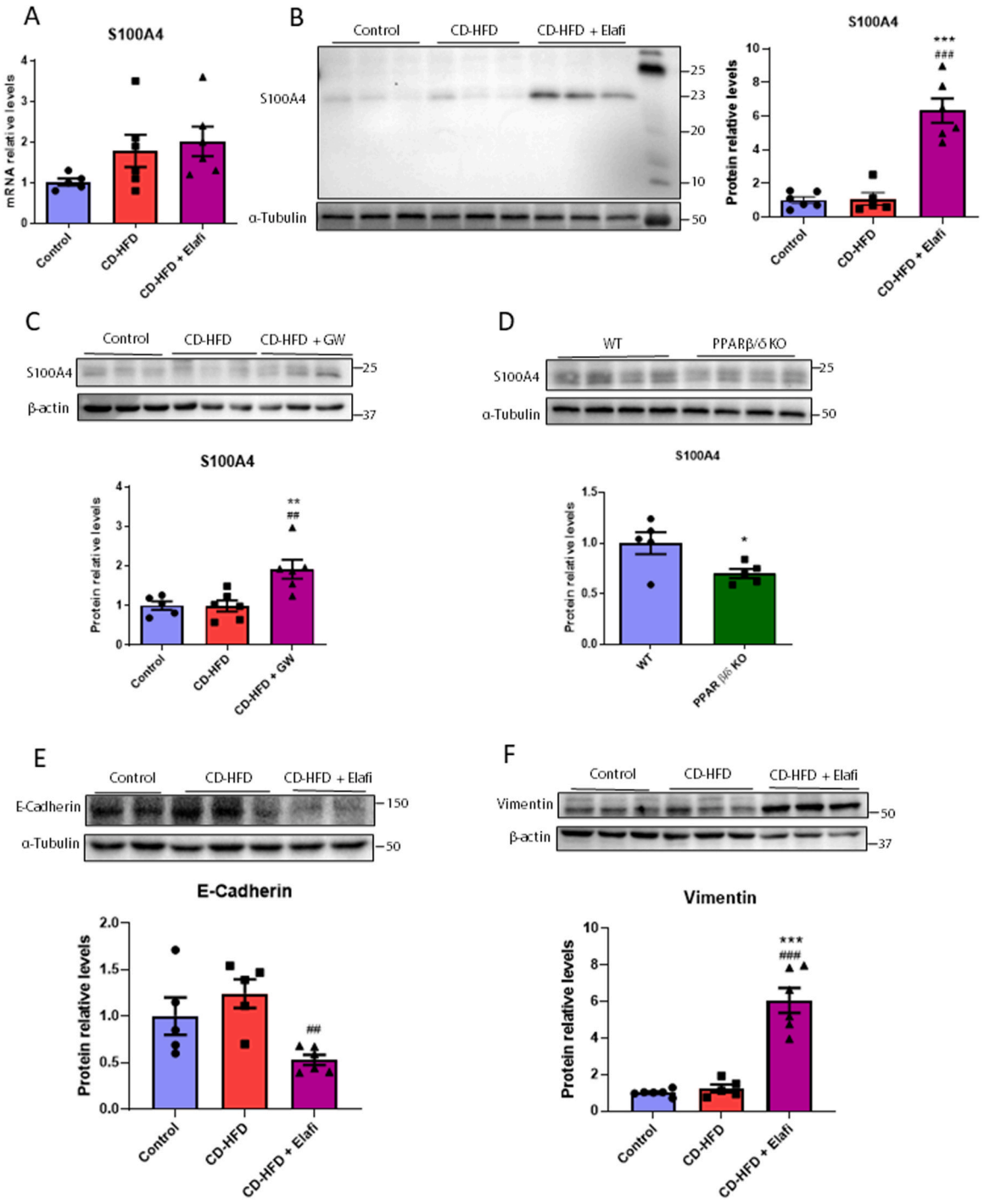

Fig. 3. Elafibranor upregulates S100A4 protein levels in the liver. (**A**) mRNA levels of *S100A4* in the livers of mice (n = 6 animals) fed a standard diet (control) or a choline-deficient high-fat diet (CD-HFD) for 12 weeks and treated with vehicle or 10 mg/kg/day of elafibranor during the last 4 weeks. (**B**) Liver cell lysate extracts were assayed via western blot analysis with antibodies against S100A4 (n = 6 animals). (**C**) S100A4 protein levels in the livers of mice (n = 6 animals) fed a standard diet (control) or a CD-HFD for 12 weeks and treated with vehicle or 5 mg/kg/day of GW501516 during the last 4 weeks. (**D**) S100A4 protein levels in the livers of WT and *Pparδ*$^{-/-}$ mice (n = 5 animals). E-cadherin (**E**) and vimentin (**F**) protein levels in the livers of mice (n = 6 animals) fed a standard diet (control) or a CD-HFD for 12 weeks and treated with vehicle or 10 mg/kg/day of elafibranor during the last 4 weeks. Data are presented as the mean ± SEM. *$p < 0.05$ and * **$p < 0.001$ versus control. $^{\#\#}p < 0.01$ and $^{\#\#\#}p < 0.001$ versus CD-HFDfed mice. p-values determined by one-way ANOVA with Tukey's post-hoc test.

treated with elafibranor (Fig. 6A). Likewise, elafibranor reduced the amount of this protein in the BRL-3A cells (Fig. 6B), and a similar behavior was observed in the mouse primary hepatocyte culture (Fig. 6C). Since ASB2α but not ASB2β induces the proteasomal degradation of filamin A [32,33], we examined the levels of filamin A in the BRL-3A cells. We observed that elafibranor did not affect filamin A levels (Fig. 6D), suggesting that this isoform of ASB2 was not affected by elafibranor, but rather the ASB2β isoform. These findings suggested that elafibranor increases S100A4 protein levels by reducing its ASB2β-mediated degradation. To confirm this, we used CRISPR/dCas9 activation plasmids designed to specifically upregulate the *Asb2* gene. Overexpression of *Asb2* (Supplementary Figure 1C-D) in the BRL-3A cells treated with vehicle reduced the basal protein levels of S100A4, confirming that this E3 ubiquitin ligase degrades S100A4 (Fig. 6E).

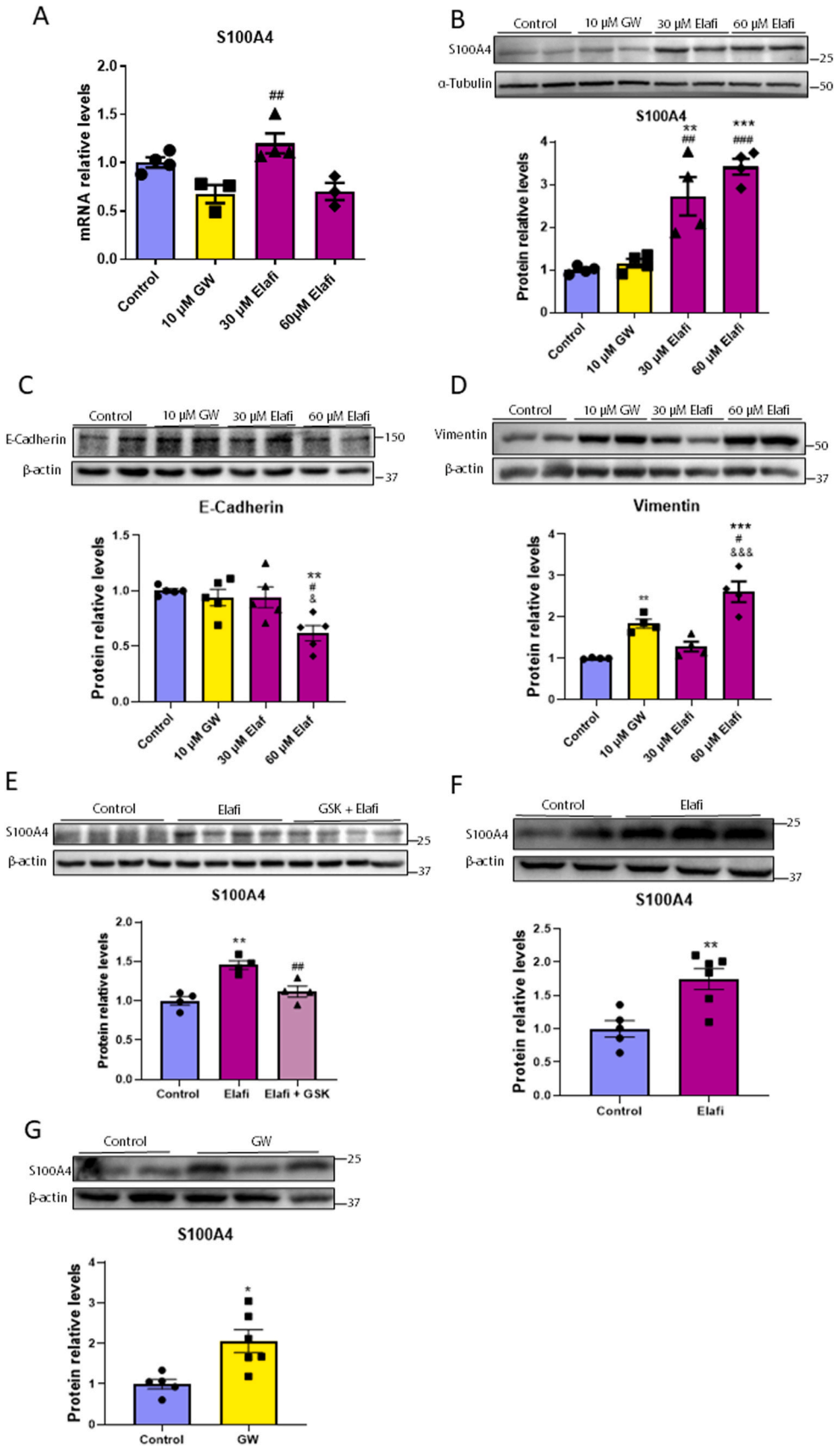

(caption on next page)

Fig. 4. Elafibranor increases S100A4 protein levels in hepatocytes. *S100A4* mRNA levels (**A**) and S100A4 protein levels (**B**) in the rat liver cell line BRL-3A exposed to 10 μM GW501516 or elafibranor (30 or 60 μM) for 24 h. E-cadherin (**C**) and vimentin (**D**) protein levels in the BRL-3A cells exposed to elafibranor (30 or 60 μM) for 24 h. S100A4 protein levels (**E**) in the BRL-3A cells exposed to 30 μM elafibranor in the presence or absence of 60 μM of the PPARβ/δ antagonist GSK0660 for 24 h. S100A4 protein levels in the mouse primary culture of hepatocytes exposed to 30 μM elafibranor (**F**) or 10 μM GW501516 (**G**) for 24 h. Data are presented as the mean ± SEM. * *$p < 0.01$ and * **$p < 0.001$ versus control. $^{\#}p < 0.05$, $^{\#\#}p < 0.01$' and $^{\#\#\#}p < 0.001$ versus GW501516-treated cells. $^{\&\&\&}p < 0.001$ versus elafibranor-treated cells p-values determined by one-way ANOVA with Tukey's post- hoc test (A-E) or two-tailed unpaired Student's t-test (F, G).

Interestingly, the increase in S100A4 levels caused by elafibranor was prevented by *Asb2* overexpression, indicating that ASB2 is involved in the effects of elafibranor on S100A4 levels. Altogether, these results suggest that elafibranor reduces the ASB2β-mediated degradation of S100A4.

4. Discussion

The development of new drugs for the treatment of MASH is challenging since findings from animal models have not been fully reproduced in clinical trials. This has also been the case of elafibranor, a drug which presented promising findings in preclinical studies, but which was discontinued in 2020 as it failed to show a statistically significant effect in patients with MASH during the phase III RESOLVE-IT clinical trial. Several factors can explain why promising preclinical drugs have failed in humans. For example, many of these compounds often target a few of the many pathways involved in the development of MASH. This limited action may result in a modest effect, or it might be attenuated by the activation of compensatory mechanisms. Therefore, no single agent is likely to control all the aspects of this complex liver disease. After the negative outcome for elafibranor in monotherapy, the efficacy of elafibranor will be evaluated in combination with other drugs for the treatment of MASH [10]. Moreover, the efficacy of this drug is also currently being examined in primary biliary cholangitis [34].

In agreement with previous studies reporting the beneficial effects of elafibranor on glucose metabolism [7], we show here that the administration of this drug to mice fed a CD-HFD, improves glucose intolerance and insulin resistance, which are among the main drivers of MASH. These changes were observed without a reduction in body weight. In addition, consistent with the findings of previous studies [35], elafibranor reduced the levels of markers of fibrosis such as α-SMA and COL1A1. Surprisingly, we observed that elafibranor increased the protein levels of S100A4, but barely affected its mRNA levels. This points to the involvement of a post-transcriptional mechanism that affects protein levels without interfering with mRNA levels. This is an unexpected finding, since S100A4 upregulation was reported to induce EMT [36], which in turn promotes fibrosis. Consistent with the role of S100A4 in liver fibrosis, S100A4-knockout mice show an attenuation in hepatic fibrosis induced by different stimuli [17,37]. S100A4 regulates the tissue fibrosis associated with type II EMT via various signaling pathways [38]. In fact, S100A4 is commonly used as a marker to identify epithelial cells undergoing EMT during tissue fibrogenesis [39], and is used as proof of EMT in hepatocytes and cholangiocytes [40–42]. In line with its induction of EMT, elafibranor upregulated the mesenchymal marker vimentin and downregulated the epithelial marker E-cadherin in the mouse liver. Moreover, the increase in S100A4 protein levels caused by elafibranor was mediated by PPARβ/δ, since an antagonist of this receptor attenuated the increase in S100A4 protein levels, while the amount of this protein was reduced in the livers of *Ppard*-null mice compared to their WT littermates. The induction of EMT in the liver by elafibranor via PPARβ/δ is in accordance with the regulation of EMT by PPARβ/δ in the human colorectal carcinoma cell line HCT116 [43]. *Ppard* knockdown in these cells upregulates E-cadherin and downregulates vimentin. Likewise, a PPARβ/δ antagonist was previously reported to block the EMT-promoting effect of stromal cell-derived factor-1 on lung cancer cells [44], while increases in EMT markers have been reported in keratinocytes by the PPARβ/δ-Src pathway [45].

The effects of PPARβ/δ on liver fibrosis are controversial. While it has been demonstrated that *Ppard*$^{-/-}$ mice show exacerbated hepatotoxicity when treated with CCl_4 [46], and that PPARβ/δ agonists attenuate hepatic fibrosis in MASLD [12], other studies have reported that these compounds enhance the proliferation of hepatic stellate cells and promote liver fibrosis [47,48]. These differences indicate that PPARβ/δ agonists may activate anti- and pro-fibrotic pathways and, depending on the model used to promote fibrosis or other factors yet to be determined, the effects of these compounds may result in either the improvement or the promotion of liver fibrosis. Given the relationship between increased S100A4 protein levels and the development of fibrosis, the increase in S100A4 protein levels and the induction of EMT might be among the factors contributing to fibrosis in mice treated with PPARβ/δ agonists. Further studies are needed to explore this possibility and to determine whether the induction of S100A4 and EMT contributes to liver fibrosis and outweighs the beneficial effects of PPARβ/δ agonists in this condition.

The present study also indicates a potential mechanism by which elafibranor increases the protein levels of S100A4. This protein is a target of ASB2, which mediates its proteasomal degradation [31]. We observed that elafibranor reduced the protein levels of ASB2 in vivo and in vitro, thereby providing an explanation for the increase in S100A4 protein levels following elafibranor treatment. In fact, *Asb2* overexpression prevented the elafibranor-mediated increase in S100A4 protein levels. Therefore, we propose that elafibranor increases S100A4 protein levels by reducing the amount of ASB2, thereby attenuating its proteasomal degradation.

S100A4 also promotes cancer progression and metastasis [17]. Although the anti-inflammatory effects of PPARβ/δ can attenuate cancer development, PPARβ/δ activation after the development of cancer can stimulate angiogenesis and tumor growth [49]. Moreover, PPARβ/δ modulation in cancer cells profoundly influences metastasis development in commonly used preclinical models in vivo [43]. It remains to be determined to what extent S100A4 upregulation by PPARβ/δ impacts cancer progression and metastasis.

Collectively, the findings of this study highlight a regulatory mechanism by which elafibranor increases the hepatic protein levels of S100A4. Further studies are needed to evaluate the consequences of the drug's induction of S100A4 and EMT, particularly in the context of MASH and cancer.

Funding

This study was partly supported by the grants RTI2018-093999-B-I00 and PID2021-122116OB-I00 (M.V-C.), PID2021-122766OB-I00 (A. M.V.), and PID2019-105989RB-I00 (J.B.) from MCIN/AEI/10.13039/501100011033 and "ERDF, A Way of Making Europe". CIBER de Diabetes y Enfermedades Metabólicas Asociadas (CIBERDEM) is a Carlos III Health Institute project. Support was also received from the CERCA Programme/Generalitat de Catalunya. Meijian Zhang was supported by a grant from the China Scholarship Council (CSC) (202007565030).

CRediT authorship contribution statement

MZ, **EB**, **MR**, **LP**, **MP**, **DAR**, **PR**, **CC**, **JJA**, **CM**, **MZ**, and **MVC** performed the experiments; **AC**, **JB**, **AMV**, **WW**, **XP**, and **MVC** analyzed the data and reviewed the results; and **MZ**, **EB**, **MR**, **LP**, and **MVC** designed the experiments and reviewed the results. **MVC** is the guarantor of this work and, as such, has full access to all the data in the study and takes

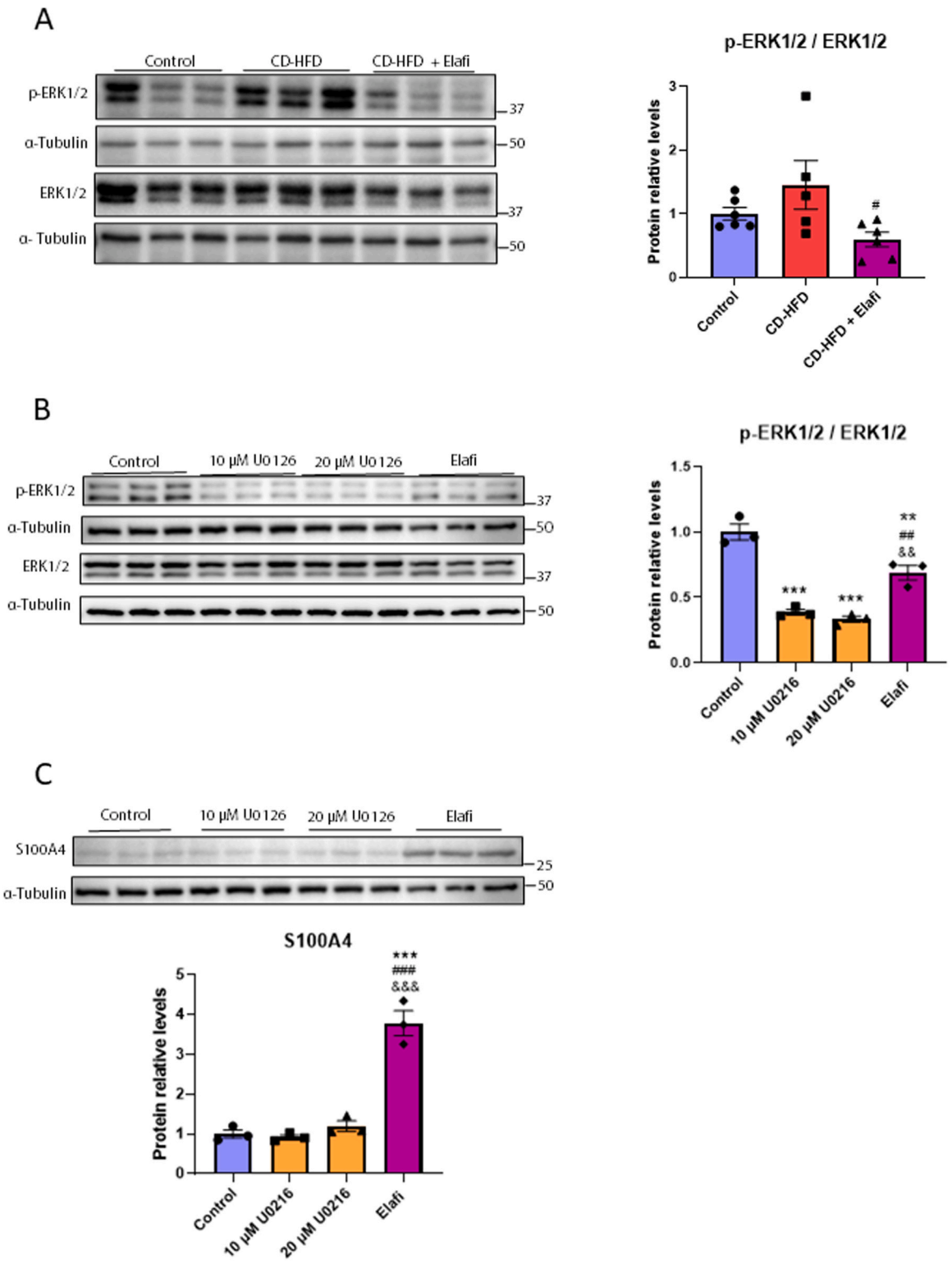

Fig. 5. ERK1/2 inhibition is not likely to be involved in the increase in S100A4 protein levels caused by elafibranor. (**A**) Total and phosphorylated ERK1/2 levels in the livers of mice (n = 6 animals) fed a standard diet (control) or a choline-deficient high-fat diet (CD-HFD) for 12 weeks and treated with vehicle or 10 mg/kg/day of elafibranor during the last 4 weeks. Total and phosphorylated ERK1/2 levels (**B**) and S100A4 protein levels (**C**) in the BRL-3A cells exposed to 60 μM elafibranor or the ERK1/2 inhibitor U0126 (10 or 20 μM). Data are presented as the mean ± SEM. $^{*}p < 0.05$, $^{* *}p < 0.01$, and $^{* **}p < 0.001$ versus control cells. $^{\#}p < 0.05$, $^{\#\#}p < 0.01$, and $^{\#\#\#}p < 0.001$ versus CD-HFD or control cells. $^{\&\&}p < 0.01$ and $^{\&\&\&}p < 0.001$ versus U0126-treated cells. p-values determined by one-way ANOVA with Tukey's post-hoc test.

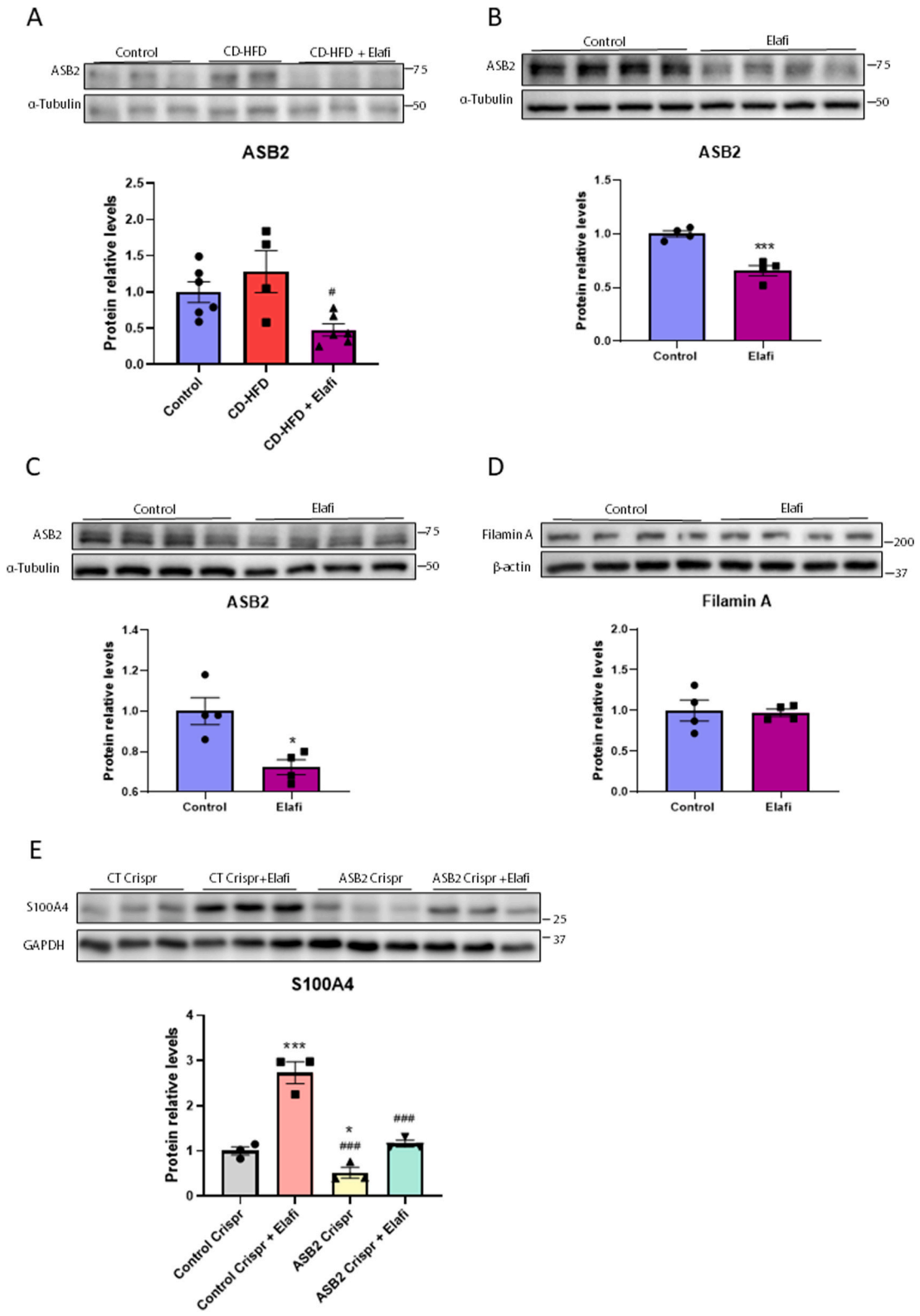

Fig. 6. ASB2 overexpression prevents the upregulation of S100A4 by elafibranor. (**A**) ASB2 protein levels in the livers of mice (n = 6 animals) fed a standard diet (control) or a choline-deficient high-fat diet (CD-HFD) for 12 weeks and treated with vehicle or 10 mg/kg/day of elafibranor during the last 4 weeks. ASB2 protein levels in the BRL-3A cells exposed to 60 μM elafibranor for 24 h (**B**) or in the mouse primary culture of hepatocytes exposed to 30 μM elafibranor for 24 h (**C**). Filamin A protein levels (**D**) in the BRL-3A cells exposed to 60 μM elafibranor for 24 h. S100A4 protein levels (**E**) in the BRL-3A cells transfected with the ASB2 CRISPR/dCas9 activation plasmids or control CRISPR/dCas9 activation plasmids and treated with either vehicle or 60 μM elafibranor for 24 h. Data are presented as the mean ± SEM. *$p < 0.05$ and * **$p < 0.001$ versus control. $^{\#}p < 0.05$ and $^{\#\#}p < 0.01$ versus CD-HFD-fed mice or CT CRISPR and elafibranor. p-values determined by one-way ANOVA with Tukey's post-hoc test (A, E) or two-tailed unpaired Student's t-test (B, C, D).

responsibility for the integrity of the data and the accuracy of the data analysis.

Declaration of Competing Interest

none`.

Data Availability

Data will be made available on request.

Acknowledgements

We would like to thank the Language Services of the University of Barcelona for revising the manuscript.

Appendix A. Supporting information

Supplementary data associated with this article can be found in the online version at doi:10.1016/j.biopha.2023.115623.

References

[1] M. Zobair, A.B.K. Younossi, Abdelatif Dinan, Fazel Yousef, Henry Linda, Wymer Mark, Global epidemiology of nonalcoholic fatty liver disease-Meta-analytic assessment of prevalence, incidence, and outcomes, Hepatology 64 (2016) 73–84.
[2] M. Machado, P. Marques-Vidal, H. Cortez-Pinto, Hepatic histology in obese patients undergoing bariatric surgery, J. Hepatol. 45 (4) (2006) 600–606.
[3] E. Buzzetti, M. Pinzani, E.A. Tsochatzis, The multiple-hit pathogenesis of non-alcoholic fatty liver disease (NAFLD), Metabolism 65 (8) (2016) 1038–1048.
[4] S.A. Sutti, E. Adaptive immunity: an emerging player in the progression of NAFLD, Nat. Rev. Gastroenterol. Hepatol. (2) (2020) 81–92.
[5] A. Suzuki, A.M. Diehl, Nonalcoholic steatohepatitis, Annu. Rev. Med. 68 (2017) 85–98.
[6] V. Ratziu, S.L. Friedman, Why do so many NASH trials fail? Gastroenterology (2020).
[7] M.J. Westerouen Van Meeteren, J.P.H. Drenth, E. Tjwa, Elafibranor: a potential drug for the treatment of nonalcoholic steatohepatitis (NASH), Expert Opin. Investig. Drugs 29 (2) (2020) 117–123.
[8] P.S. Dulai, S. Singh, J. Patel, M. Soni, L.J. Prokop, Z. Younossi, G. Sebastiani, M. Ekstedt, H. Hagstrom, P. Nasr, P. Stal, V.W. Wong, S. Kechagias, R. Hultcrantz, R. Loomba, Increased risk of mortality by fibrosis stage in nonalcoholic fatty liver disease: Systematic review and meta-analysis, Hepatology 65 (5) (2017) 1557–1565.
[9] GENFIT. Announces Results from Interim Analysis of RESOLVE-IT Phase 3 Trial of Elafibranor in Adults with NASH and Fibrosis. https://ml-eu.globe newsw ire.com/Resource/Downl oad/38e08 5e1–66f5–4251-8abe-648d0 e7b9e d1; Press release (2020). In.
[10] NASH Ei. https://www.genfi t.com/pipel ine/elafibranor/ (2020). In.
[11] B. Staels, A. Rubenstrunk, B. Noel, G. Rigou, P. Delataille, L.J. Millatt, M. Baron, A. Lucas, A. Tailleux, D.W. Hum, V. Ratziu, B. Cariou, R. Hanf, Hepatoprotective effects of the dual peroxisome proliferator-activated receptor alpha/delta agonist, GFT505, in rodent models of nonalcoholic fatty liver disease/nonalcoholic steatohepatitis, Hepatology 58 (6) (2013) 1941–1952.
[12] K. Iwaisako, M. Haimerl, Y.H. Paik, K. Taura, Y. Kodama, C. Sirlin, E. Yu, R.T. Yu, M. Downes, R.M. Evans, D.A. Brenner, B. Schnabl, Protection from liver fibrosis by a peroxisome proliferator-activated receptor delta agonist, Proc. Natl. Acad. Sci. USA 109 (21) (2012) E1369–E1376.
[13] M. Zarei, J. Pizarro-Delgado, E. Barroso, X. Palomer, M. Vazquez-Carrera, Targeting FGF21 for the treatment of nonalcoholic steatohepatitis, Trends Pharm. Sci. 41 (3) (2020) 199–208.
[14] N. Wagner, K.D. Wagner, PPAR beta/delta and the hallmarks of cancer, Cells 9 (5) (2020).
[15] R. Kalluri, R.A. Weinberg, The basics of epithelial-mesenchymal transition, J. Clin. Investig. 119 (6) (2009) 1420–1428.
[16] Y. Li, J. Wang, K. Song, S. Liu, H. Zhang, F. Wang, C. Ni, W. Zhai, J. Liang, Z. Qin, J. Zhang, S100A4 promotes hepatocellular carcinogenesis by intensifying fibrosis-associated cancer cell stemness, Oncoimmunology 9 (1) (2020), 1725355.
[17] D.M. Helfman, E.J. Kim, E. Lukanidin, M. Grigorian, The metastasis associated protein S100A4: role in tumour progression and metastasis, Br. J. Cancer 92 (11) (2005) 1955–1958.
[18] S.C. Garrett, K.M. Varney, D.J. Weber, A.R. Bresnick, S100A4, a mediator of metastasis, J. Biol. Chem. 281 (2) (2006) 677–680.
[19] L. Santamaria-Kisiel, A.C. Rintala-Dempsey, G.S. Shaw, Calcium-dependent and -independent interactions of the S100 protein family, Biochem J. 396 (2) (2006) 201–214.
[20] M. Tsuchiya, F. Yamaguchi, S. Shimamoto, T. Fujimoto, H. Tokumitsu, M. Tokuda, R. Kobayashi, Oxidized S100A4 inhibits the activation of protein phosphatase 5 through S100A1 in MKN-45 gastric carcinoma cells, Int J. Mol. Med 34 (6) (2014) 1713–1719.
[21] Y. Takahashi, Y. Soejima, T. Fukusato, Animal models of nonalcoholic fatty liver disease/nonalcoholic steatohepatitis, World J. Gastroenterol. 18 (19) (2012) 2300–2308.
[22] M.V. Chakravarthy, I.J. Lodhi, L. Yin, R.R. Malapaka, H.E. Xu, J. Turk, C. F. Semenkovich, Identification of a physiologically relevant endogenous ligand for PPARalpha in liver, Cell 138 (3) (2009) 476–488.
[23] E. Barroso, R. Rodriguez-Calvo, L. Serrano-Marco, A.M. Astudillo, J. Balsinde, X. Palomer, M. Vazquez-Carrera, The PPARbeta/delta activator GW501516 prevents the down-regulation of AMPK caused by a high-fat diet in liver and amplifies the PGC-1alpha-Lipin 1-PPARalpha pathway leading to increased fatty acid oxidation, Endocrinology 152 (5) (2011) 1848–1859.
[24] M. Zarei, D. Aguilar-Recarte, X. Palomer, M. Vazquez-Carrera, Revealing the role of peroxisome proliferator-activated receptor beta/delta in nonalcoholic fatty liver disease, Metabolism 114 (2021), 154342.
[25] V.N. Malashkevich, N.G. Dulyaninova, U.A. Ramagopal, M.A. Liriano, K. M. Varney, D. Knight, M. Brenowitz, D.J. Weber, S.C. Almo, A.R. Bresnick, Phenothiazines inhibit S100A4 function by inducing protein oligomerization, Proc. Natl. Acad. Sci. USA 107 (19) (2010) 8605–8610.
[26] T. Tanaka, J. Yamamoto, S. Iwasaki, H. Asaba, H. Hamura, Y. Ikeda, M. Watanabe, K. Magoori, R.X. Ioka, K. Tachibana, Y. Watanabe, Y. Uchiyama, K. Sumi, H. Iguchi, S. Ito, T. Doi, T. Hamakubo, M. Naito, J. Auwerx, M. Yanagisawa, T. Kodama, J. Sakai, Activation of peroxisome proliferator-activated receptor delta induces fatty acid beta-oxidation in skeletal muscle and attenuates metabolic syndrome, Proc. Natl. Acad. Sci. USA 100 (26) (2003) 15924–15929.
[27] R.P. House, M. Pozzuto, P. Patel, N.G. Dulyaninova, Z.H. Li, W.D. Zencheck, M. I. Vitolo, D.J. Weber, A.R. Bresnick, Two functional S100A4 monomers are necessary for regulating nonmuscle myosin-IIA and HCT116 cell invasion, Biochemistry 50 (32) (2011) 6920–6932.
[28] R.R. Bowers, Y. Manevich, D.M. Townsend, K.D. Tew, Sulfiredoxin redox-sensitive interaction with S100A4 and non-muscle myosin IIA regulates cancer cell motility, Biochemistry 51 (39) (2012) 7740–7754.
[29] R. Zakaria, I. Lamsoul, S. Uttenweiler-Joseph, M. Erard, B. Monsarrat, O. Burlet-Schiltz, C. Moog-Lutz, P.G. Lutz, Phosphorylation of serine 323 of ASB2alpha is pivotal for the targeting of filamin A to degradation, Cell Signal 25 (12) (2013) 2823–2830.
[30] R. Rodriguez-Calvo, L. Serrano, T. Coll, N. Moullan, R.M. Sanchez, M. Merlos, X. Palomer, J.C. Laguna, L. Michalik, W. Wahli, M. Vazquez-Carrera, Activation of peroxisome proliferator-activated receptor beta/delta inhibits lipopolysaccharide-induced cytokine production in adipocytes by lowering nuclear factor-kappaB activity via extracellular signal-related kinase 1/2, Diabetes 57 (8) (2008) 2149–2157.
[31] S. Braumann, T. Thottakara, S. Stucker, S. Reischmann-Dusener, E. Kramer, J. Gross, M.N. Hirt, S. Doroudgar, L. Carrier, F.W. Friedrich, S100A4 as a target of the E3-ligase Asb2beta and its effect on engineered heart tissue, Front. Physiol. 9 (2018), 1292.
[32] N.F. Bello, I. Lamsoul, M.L. Heuze, A. Metais, G. Moreaux, D.A. Calderwood, D. Duprez, C. Moog-Lutz, P.G. Lutz, The E3 ubiquitin ligase specificity subunit ASB2beta is a novel regulator of muscle differentiation that targets filamin B to proteasomal degradation, Cell Death Differ. 16 (6) (2009) 921–932.
[33] M.L. Heuze, I. Lamsoul, M. Baldassarre, Y. Lad, S. Leveque, Z. Razinia, C. Moog-Lutz, D.A. Calderwood, P.G. Lutz, ASB2 targets filamins A and B to proteasomal degradation, Blood 112 (13) (2008) 5130–5140.
[34] J.M. Schattenberg, A. Pares, K.V. Kowdley, M.A. Heneghan, S. Caldwell, D. Pratt, A. Bonder, G.M. Hirschfield, C. Levy, J. Vierling, D. Jones, A. Tailleux, B. Staels, S. Megnien, R. Hanf, D. Magrez, P. Birman, V. Luketic, A randomized placebo-controlled trial of elafibranor in patients with primary biliary cholangitis and incomplete response to UDCA, J. Hepatol. 74 (6) (2021) 1344–1354.
[35] A.M. van den Hoek, L. Verschuren, M.P.M. Caspers, N. Worms, A.L. Menke, H.M. G. Princen, Beneficial effects of elafibranor on NASH in E3L.CETP mice and differences between mice and men, Sci. Rep. 11 (1) (2021), 5050.
[36] L. Song, T.Y. Chen, X.J. Zhao, Q. Xu, R.Q. Jiao, J.M. Li, L.D. Kong, Pterostilbene prevents hepatocyte epithelial-mesenchymal transition in fructose-induced liver fibrosis through suppressing miR-34a/Sirt1/p53 and TGF-beta1/Smads signalling, Br. J. Pharmacol. 176 (11) (2019) 1619–1634.
[37] L. Chen, J. Li, J. Zhang, C. Dai, X. Liu, J. Wang, Z. Gao, H. Guo, R. Wang, S. Lu, F. Wang, H. Zhang, H. Chen, X. Fan, S. Wang, Z. Qin, S100A4 promotes liver fibrosis via activation of hepatic stellate cells, J. Hepatol. 62 (1) (2015) 156–164.
[38] F. Fei, J. Qu, C. Li, X. Wang, Y. Li, S. Zhang, Role of metastasis-induced protein S100A4 in human non-tumor pathophysiologies, Cell Biosci. 7 (2017), 64.
[39] M. Iwano, D. Plieth, T.M. Danoff, C. Xue, H. Okada, E.G. Neilson, Evidence that fibroblasts derive from epithelium during tissue fibrosis, J. Clin. Investig. 110 (3) (2002) 341–350.
[40] M. Zeisberg, C. Yang, M. Martino, M.B. Duncan, F. Rieder, H. Tanjore, R. Kalluri, Fibroblasts derive from hepatocytes in liver fibrosis via epithelial to mesenchymal transition, J. Biol. Chem. 282 (32) (2007) 23337–23347.
[41] A. Omenetti, A. Porrello, Y. Jung, L. Yang, Y. Popov, S.S. Choi, R.P. Witek, G. Alpini, J. Venter, H.M. Vandongen, W.K. Syn, G.S. Baroni, A. Benedetti, D. Schuppan, A.M. Diehl, Hedgehog signaling regulates epithelial-mesenchymal transition during biliary fibrosis in rodents and humans, J. Clin. Investig. 118 (10) (2008) 3331–3342.
[42] K.A. Rygiel, H. Robertson, H.L. Marshall, M. Pekalski, L. Zhao, T.A. Booth, D. E. Jones, A.D. Burt, J.A. Kirby, Epithelial-mesenchymal transition contributes to portal tract fibrogenesis during human chronic liver disease, Lab Investig. 88 (2) (2008) 112–123.

[43] X. Zuo, W. Xu, M. Xu, R. Tian, M.J. Moussalli, F. Mao, X. Zheng, J. Wang, J. S. Morris, M. Gagea, C. Eng, S. Kopetz, D.M. Maru, A. Rashid, R. Broaddus, D. Wei, M.C. Hung, A.K. Sood, I. Shureiqi, Metastasis regulation by PPARD expression in cancer cells, JCI Insight 2 (1) (2017), e91419.
[44] Y. Wang, W. Lan, M. Xu, J. Song, J. Mao, C. Li, X. Du, Y. Jiang, E. Li, R. Zhang, Q. Wang, Cancer-associated fibroblast-derived SDF-1 induces epithelial-mesenchymal transition of lung adenocarcinoma via CXCR4/beta-catenin/PPARdelta signalling. Cell Death Dis. 12 (2) (2021), 214.
[45] A. Montagner, M.B. Delgado, C. Tallichet-Blanc, J.S. Chan, M.K. Sng, H. Mottaz, G. Degueurce, Y. Lippi, C. Moret, M. Baruchet, M. Antsiferova, S. Werner, D. Hohl, T.A. Saati, P.J. Farmer, N.S. Tan, L. Michalik, W. Wahli, Src is activated by the nuclear receptor peroxisome proliferator-activated receptor beta/delta in ultraviolet radiation-induced skin cancer, EMBO Mol. Med. 6 (1) (2014) 80–98.
[46] W. Shan, C.J. Nicol, S. Ito, M.T. Bility, M.J. Kennett, J.M. Ward, F.J. Gonzalez, J. M. Peters, Peroxisome proliferator-activated receptor-beta/delta protects against chemically induced liver toxicity in mice. Hepatology 47 (1) (2008) 225–235.
[47] K. Hellemans, L. Michalik, A. Dittie, A. Knorr, K. Rombouts, J. De Jong, C. Heirman, E. Quartier, F. Schuit, W. Wahli, A. Geerts, Peroxisome proliferator-activated receptor-beta signaling contributes to enhanced proliferation of hepatic stellate cells. Gastroenterology 124 (1) (2003) 184–201.
[48] R. Kostadinova, A. Montagner, E. Gouranton, S. Fleury, H. Guillou, D. Dombrowicz, P. Desreumaux, W. Wahli, GW501516-activated PPARbeta/delta promotes liver fibrosis via p38-JNK MAPK-induced hepatic stellate cell proliferation, Cell Biosci. 2 (1) (2012), 34.
[49] J.M. Peters, F.J. Gonzalez, R. Muller, Establishing the role of PPARbeta/delta in carcinogenesis, Trends Endocrinol. Metab. 26 (11) (2015) 595–607.
[50] K. Nadra, S.I. Anghel, E. Joye, N.S. Tan, S. Basu-Modak, D. Trono, W. Wahli, B. Desvergne, Differentiation of trophoblast giant cells and their metabolic functions are dependent on peroxisome proliferator-activated receptor beta/delta, Mol. Cell Biol. 26 (8) (2006) 3266–3281.
[51] J.C. McGrath, E. Lilley, Implementing guidelines on reporting research using animals (ARRIVE etc.): new requirements for publication in BJP, Br. J. Pharmacol. 172 (13) (2015) 3189–3193.
[52] E.G. Bligh, W.J. Dyer, A rapid method of total lipid extraction and purification, Can. J. Biochem. Physiol. 37 (8) (1959) 911–917.
[53] D. Balgoma, A.M. Astudillo, G. Perez-Chacon, O. Montero, M.A. Balboa, J. Balsinde, Markers of monocyte activation revealed by lipidomic profiling of arachidonic acid-containing phospholipids, J. Immunol. 184 (7) (2010) 3857–3865.
[54] R. Benveniste, T.M. Danoff, J. Ilekis, H.R. Craig, Epidermal growth factor receptor numbers in male and female mouse primary hepatocyte cultures, Cell Biochem. Funct. 6 (4) (1988) 231–235.
[55] L. Salvado, E. Barroso, A.M. Gomez-Foix, X. Palomer, L. Michalik, W. Wahli, M. Vazquez-Carrera, PPARbeta/delta prevents endoplasmic reticulum stress-associated inflammation and insulin resistance in skeletal muscle cells through an AMPK-dependent mechanism, Diabetologia 57 (10) (2014) 2126–2135.